

# Thermochemical Review of Jarosite and Goethite Stability Regions at 25 and 95°C

Cüneyt ARSLAN

*Istanbul Technical University, Metallurgical and Materials Engineering Department,  
80626 Maslak, İstanbul-TURKEY  
arslanc@itu.edu.tr*

Fatma ARSLAN

*Istanbul Technical University, Mining Engineering Department,  
80626 Maslak, İstanbul-TURKEY*

Received 30.11.2001

## Abstract

The hydrometallurgical treatment of zinc sulfide concentrates involves the separation of zinc from iron, since most zinc concentrates contain 5-12% iron. Several processes, such as hematite, magnetite, goethite and jarosite, have been developed for the removal of iron from solution prior to zinc electrolysis. The precipitation of iron is controlled by a set of thermodynamic and kinetic factors operative both in iron solutions and in precipitates. Identifying these factors and their relations is important for the control of these processes. In brief, thermodynamic stability regions of iron compounds formed during the jarosite and goethite processes, which are commercially used in the zinc industry, are outlined in this paper.

**Key words:** Jarosite, Goethite, Iron Precipitation, Solution Purification

## Introduction

The electrolytic zinc process is one of today's most successful hydrometallurgical operations. In this process, zinc sulfide concentrates are roasted and acid leached, then the zinc is electrowon after solution purification (Brown, 1971; Arregui *et al.*, 1979; Dutrizac, 1980). There has been interest in processing zinc sulfide materials by direct acidic leaching under oxidizing conditions. By this process, sulfur can be produced in the elemental form, rather than as SO<sub>2</sub>, and the process can be more efficient and cost-effective than conventional treatment and is suitable for mixed sulfides that cannot be conveniently treated by the roasting and leaching process (Arregui *et al.*, 1979; Dutrizac, 1980). Commercial methods were implemented by Cominco and Kidd Creek Mines in Canada, both of which integrated pressure leaching with their conventional electrolytic zinc plants to increase their overall plant capacities

(Sheritt-Gordon Mines Ltd., 1977).

The hydrometallurgical treatment of zinc sulfide concentrates has always been concerned with the separation of zinc from iron. This arises from the fact that most zinc concentrates contain iron, some in significant proportions (from 5 to 12%). Prior to the hydrometallurgical treatment of a zinc concentrate, it is usually necessary to employ a roasting step. During roasting of the zinc concentrates most of the iron present in the concentrate combines with zinc oxide to form zinc ferrite (ZnO·Fe<sub>2</sub>O<sub>3</sub>). Neutral leaching of the roasted concentrate (calcine) ends up with the dissolution of free zinc oxide as ZnSO<sub>4</sub>, but the zinc trapped in zinc ferrite will not be leached very significantly. Although hot sulfuric acid leaching can liberate the zinc in the ferrite, iron associated with zinc also dissolves.

The simple neutralization of the sulfate solution is not recommended due to the formation of a gelatinous ferric hydroxide precipitation, which seriously

interferes with thickening, filtering, and washing operations and includes a significant amount of zinc (Umetsu *et al.*, 1976). The hydrometallurgical recovery of zinc in ferrite became commercially feasible only after the development of effective iron precipitation techniques. For many years, the recovery of zinc in the electrolytic process was restricted in those cases where there was a significant portion of iron in the zinc concentrates treated. Research is still continuing on the removal of iron from zinc electrolytes (Dutrizac, 1999; Dutrizac, 2000; Acharya *et al.*, 1992; Principe and Demopoulos, 1999). The need for economic ways of removing high concentrations of iron from solution was met by the development of several processes, such as the hematite, goethite, magnetite, and jarosite processes (Brown, 1971; Arregui *et al.*, 1979; Dutrizac, 1980; McAndrew *et al.*, 1975). The hematite process is a more recent innovation in the zinc industry although the precipitation of iron as  $\text{Fe}_2\text{O}_3$  at elevated temperatures and pressures has been known for some time. The commercial application of the hematite process was practiced by the Akita Zinc Company in Japan (Tsunoda *et al.*, 1973).

Although the magnetite process has yet to find a commercial application in the zinc industry, variations of it have long been used for both the preparation of brown-black paint pigments and for the synthesis of ferrites for diverse electronic applications. The application of the technique to metallur-

gical process streams, such as iron-containing zinc solutions from the hydrometallurgical treatment of sphalerite, was suggested by Sheritt-Gordon Mines Limited (1977). The goethite process, another approach to eliminating the iron problem, was developed by Societe de la Vieille Montagne of Belgium (1972) and the Electrolytic Zinc Company of Australasia (Delvaux, 1976) later in the 1960s, and commercially used. In this process, iron can be precipitated as an easily filterable form, crystalline goethite,  $\text{FeOOH}$  (Arregui *et al.*, 1976; Dutrizac, 1980; Societe de la Vieille Montagne, 1972).

The jarosite process, which has proved to be the most widely adopted (Brown, 1971; Arregui *et al.*, 1976; Dutrizac, 1980; Kershaw and Pickering, 1980; Arauco and Doyle, 1986), was developed in the mid 1960s by Austriana de Zinc S.A. of Spain (1969), Det Norske Zinkkompani A/S of Norway (1969), and Electrolytic Zinc Company of Australasia Ltd. (1970), independently. The electrolytic zinc plants using the jarosite process are listed in Table 1 (Arregui *et al.*, 1976).

There are several flowsheets for the application of the jarosite process followed around the world. The simplest two-stage jarosite precipitation flowsheet is shown in Figure 1, and other processes have been evolved that include multiple stage leaching, preneutralization, jarosite leaching, silver-lead residue recovery etc. (Dutrizac, 1980).

**Table 1.** Plants using jarosite process and their nominal capacities (Arregui *et al.*, 1979).

Company Capacity (t/year)	Country	Holland
Austriana de Zinc S.A.	Spain	200,000
Budelco	Holland	150,000
Canadian Electrolytic Zinc	Canada	205,000
Compagnie Royale Asturienne des Mines	France	120,000
Electrolytic Zinc Company of Australasia Ltd.	Australia	210,000
Hemisjka Industrija Zorka	Yugoslavia	30,000
Korea Zinc	Korea	50,000
Met Mex Penoles	Mexico	100,000
Norzink AS	Norway	85,000
Outokumpu Oy	Finland	160,000
Preussag-Weser-Zink	Germany	110,000
Sulfacid	Argentina	30,000
Societe de Prayon	Belgium	60,000
Texasgulf	Canada	120,000
Toho Zinc	Japan	140,000

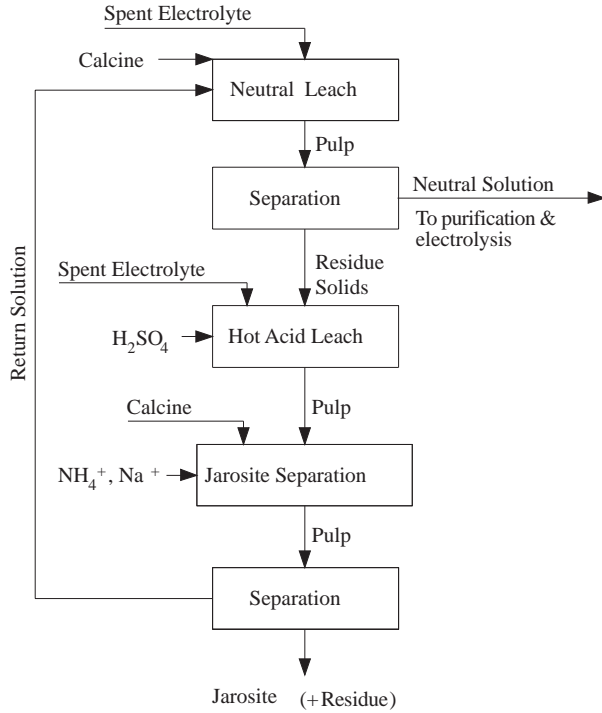
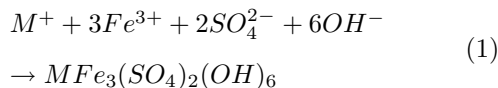


**Figure 1.** Simple two-stage jarosite precipitation (Dutrizac, 1980).

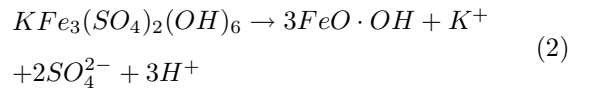
The main advantage of precipitating jarosite-type compounds is comparative ease of settling, filtration, and washing of the residue; iron gels are therefore avoided. At the same time, its use enables a very significant improvement in the efficient use of zinc concentrates, together with improved recoveries of associated metals such as lead, silver, gold, copper, and cadmium. The process has been further improved to give even higher recoveries of zinc and other metals and it is now possible to produce a purer jarosite, which facilitates recovery of its iron content as well as making it more acceptable for disposal by other routes. The “clean” jarosite produced by the new procedures may allow the production of material suitable for iron manufacture (Hage *et al.*, 1999). The procedures include calcining, sintering, and thermal hydrolysis and in all cases where iron oxides are formed. Jarosite processing wastes may also be used as construction materials (Li and Hao, 1999).

The precipitation of jarosite can generally be written as (Dutrizac, 1980):



where M can be  $K^+$ ,  $Na^+$ ,  $H_3O^+$ ,  $NH_4^+$ ,  $Pb^{2+}$ , etc.. Hydroxyl concentration (i.e., pH) exercises a major effect on iron removal as jarosite. Temperature and especially pH are the most important control variables, with the restriction that the pH must remain below about 1.8-2.0 to prevent precipitation of other iron phases. High temperatures can be used to counteract high acidities. For a given pH and iron and sulfate concentration, K-jarosite  $[KFe_3(SO_4)_2(OH)_6]$  is the least soluble, followed by the sodium and ammonium jarosite compounds.

The conversion of jarosite to goethite is relatively unfavorable (Brown, 1971):



and this decomposition route is unlikely, at least for K-, Na-, and  $NH_4^+$ -jarosites.

In the abovementioned iron precipitation processes, the precipitation of iron is controlled by a complex set of thermodynamic and kinetic factors operative both in the iron solutions and in precipitates. It is important that these factors and their relations be identified so that these processes can be controlled.

The purpose of this paper is to outline the thermodynamic stability regions of iron compounds formed during the jarosite and goethite processes, which are commercially used in the zinc industry. Room temperature (25°C) and 95°C are selected in this study, since the precipitation of jarosite at 90-95°C was found to be more effective with potassium ions than with ammonium ions, sodium ions being the least effective of the three (Arregui *et al.*, 1976).

## Calculations

The equilibrium relationships between ionic iron species or compounds were demonstrated by calculating Eh-pH diagrams at two different temperatures (25 and 95°C). Eh-pH diagrams considering goethite and K-jarosite compounds were simply reproduced from their originals drawn by using a computer program developed by Duby (1976) for constructing potential-pH diagrams, and can be used to predict the conditions required for precipitating various compounds.

**Table 2.** Thermodynamic data of some species involved in the Fe-H<sub>2</sub>O-S system.

Compounds	$\Delta G_f^\circ$ (298K) (kcal/mol)	Ref.	Entropy (298K) (cal/mol)	Ref.	Heat capacity	Ref.	$\Delta G_f^\circ$ (368K) (kcal/mol)
Fe	0.0	[NBS]]	6.52	[NBS]]	$5.45+2.02 \times 10^{-3} T$	[BKK]	-5.037
Fe <sup>2+</sup>	-18.85	[NBS]]	-32.9	[NBS]]	70	[CC]	-17.078
Fe <sup>3+</sup>	-1.1	[NBS]]	-75.5	[NBS]]	93	[CC]	3.4744
FeOH <sup>++</sup>	-54.83	[NBS]]	-7.0	[NBS]]	64	[CC]	-54.763
Fe(OH) <sub>2</sub> <sup>+</sup>	-104.7	[NBS]]	17.2	[K]	$27.137-4.737 \times 10^{-3} T-5 \times 10^5 / T^2$	[K]	-106.07
Fe(OH) <sub>2</sub>	-116.3	[NBS]]	21.0	[NBS]]	$27.422-5.022 \times 10^{-3} T-5 \times 10^5 / T^2$	[K]	-117.94
Fe(OH) <sub>2</sub> <sup>-</sup>	-157.501	[SM]	25.2	[K]	$29.132-6.73 \times 10^{-3} T-5 \times 10^5 / T^2$	[K]	-159.44
FeOH <sup>+</sup>	-66.3	[NBS]]	-7.0	[K]	53	[CC]	-66.2119
Fe <sub>2</sub> (OH) <sub>2</sub> <sup>4+</sup>	-111.68	[NBS]]	-85.0	[NBS]]	$7+2.13 \times 10^{-2} T+6 \times 10^5 / T^2$	[K]	-105.877
Fe(OH) <sub>3</sub>	-166.5	[NBS]]	25.5	[NBS]]	$37.13-7.23 \times 10^{-3} T-7 \times 10^5 / T^2$	[K]	-168.492
HFeO <sub>2</sub> <sup>-</sup>	-90.3	[NBS]]	12.0	[K]	$18.176+7.124 \times 10^{-3} T-4 \times 10^5 / T^2$	[K]	-91.276
Fe <sub>2</sub> O <sub>3</sub>	-177.4	[NBS]]	20.89	[K]	$23.49+18.6 \times 10^{-3} T-3.55 \times 10^{-5} / T^2$	[BKK]	-179.094
FeO <sub>4</sub> <sup>2-</sup>	-111.0	[GC]	19.8	[K]	$26.563+5.237 \times 10^{-3} T-5 \times 10^5 / T^2$	[K]	-112.5755
Fe <sub>3</sub> O <sub>4</sub>	-242.7	[NBS]]	35.0	[K]	$21.88+48.2 \times 10^{-3} T$	[BKK]	-245.45
FeO	-58.595	[NBS]]	13.74	[K]	$12.38+1.62 \times 10^{-3} T-0.38 \times 10^{-5} / T^2$	[BKK]	-59.6559
FeOOH	-110.418	[SM]	14.2	[BKK]	$22.857+1.428 \times 10^{-4} T-4 \times 10^5 / T^2$	[K]	-111.56
FeSO <sub>4</sub>	-196.82	[NBS]]	-28.1	[NBS]]	$26.65+1.475 \times 10^{-2} T-6 \times 10^5 / T^2$	[K]	-195.064
FeS	-24.0	[NBS]]	14.41	[NBS]]	$5.19+26.4 \times 10^{-3} T$	[BKK]	-25.123
FeS <sub>2</sub>	-39.9	[NBS]]	12.65	[NBS]]	$17.88+1.32 \times 10^{-3} T-3.05 \times 10^{-5} / T^2$	[BKK]	-40.926
Na <sup>+</sup>	-62.593	[NBS]]	14.1	[NBS]]	37	[CC]	-63.86
SO <sub>4</sub> <sup>2-</sup>	-177.97	[NBS]]	4.8	[NBS]]	-108	[CC]	-177.84
HSO <sub>4</sub> <sup>-</sup>	-180.69	[NBS]]	31.5	[NBS]]	-10	[CC]	-182.82
S <sup>2-</sup>	20.5	[NBS]]	-3.5	[NBS]]	-58	[CC]	21.108
HS <sup>-</sup>	2.88	[NBS]]	15.0	[NBS]]	-58	[CC]	2.273
H <sub>2</sub> S	-6.66	[NBS]]	29.0	[NBS]]	$10.9+8.3 \times 10^{-3} T-3 \times 10^5 / T^2$	[K]	-8.72
SO <sub>3</sub> <sup>2-</sup>	-116.3	[NBS]]	-7.0	[NBS]]	-132	[CC]	-114.8
HSO <sub>3</sub> <sup>-</sup>	-126.15	[NBS]]	-33.4	[NBS]]	-11	[CC]	-128.4
K <sup>+</sup>	-67.7	[NBS]]	24.5	[NBS]]	35	[CC]	-69.68
KSO <sub>4</sub> <sup>2-</sup>	-246.69	[NBS]]	36.1	[NBS]]	28	[CC]	-248.864
K-Jarosite	-788.6	[D]	110.4	[K]	$129.853+10^{-2} T-26 \times 10^5 / T^2$	[K]	-797.202
H-Jarosite	-772.5	[D]	61.435	[K]	$116.145+8.06 \times 10^{-2} T-29 \times 10^5 / T^2$	[K]	-777.75

[NBS]: NBS, 1982.

[BKK]: Barin et al., 1977.

[SM]: Stumm &amp; Morgan, 1981.

[GC]: Garrels &amp; Christ, 1965

[CC]: Criss &amp; Cobble, 1964.

[D]: Dutrizac, 1980.

[K]: Kellogg, 1988.

Most of the required thermodynamic data for the calculations were taken from NBS series (NBS, 1982). However, since there was no data available for elevated temperatures, the ‘‘Entropy Correspondence Principle’’, suggested by Criss & Cobble (1964), was employed for estimating the free energy of formation of the compounds. Kellogg’s estimation procedure (1988) was also used for those compounds whose entropy and heat capacity values could not be found. All the thermodynamic values and estimations are listed in Table 2. The presented Eh-pH diagrams can be categorized into three groups:

### 1. Stability Region of K-Jarosite:

at 298K:

- with Fe<sub>2</sub>O<sub>3</sub> (Figure 2)
- with Fe<sub>2</sub>O<sub>3</sub> and Fe(OH)<sub>2</sub><sup>-</sup> (Figure 3)
- with Fe(OH)<sub>2</sub><sup>-</sup> (Figure 4)

at 368K:

- with Fe<sub>2</sub>O<sub>3</sub> (Figure 5)
- with Fe<sub>2</sub>O<sub>3</sub> and Fe(OH)<sub>2</sub><sup>-</sup> (Figure 6)
- with Fe(OH)<sub>2</sub><sup>-</sup> (Figure 7)

### 2. Stability Region of Goethite:

at 298K:

- without Fe<sub>2</sub>O<sub>3</sub> and Fe(OH)<sub>2</sub><sup>-</sup> (Figure 8)
- without Fe<sub>2</sub>O<sub>3</sub> (Figure 9)

at 368K:

- without Fe<sub>2</sub>O<sub>3</sub> and Fe(OH)<sub>2</sub><sup>-</sup> (Figure 10)
- without Fe<sub>2</sub>O<sub>3</sub> (Figure 11)

### 3. Stability Region of K-Jarosite and Goethite:

- at 298K without Fe<sub>2</sub>O<sub>3</sub> (Figure 12)
- at 368K without Fe<sub>2</sub>O<sub>3</sub> (Figure 13)

Each of the diagrams was actually drawn for eight different activity combinations of the involving species. Selected activity values were:

$$\begin{aligned} \text{For [Fe]} &= 1.0 \quad \text{or} \quad 0.1, \\ \text{For [S]} &= 1.0 \quad \text{or} \quad 0.1, \quad \text{and} \\ \text{For [K]} &= 0.1 \quad \text{or} \quad 0.01 \end{aligned}$$

Illustrated diagrams were drawn for the case where iron and sulfur activities were equal to 1.0, whereas the activity of K was equal to 0.1.

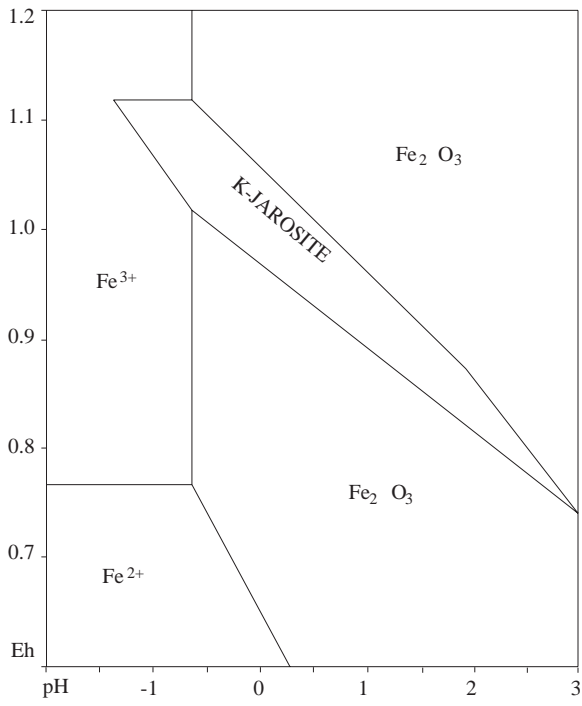


**Figure 2.** Stability region of K-jarosite at 298K (with the existence of Fe<sub>2</sub>O<sub>3</sub>).

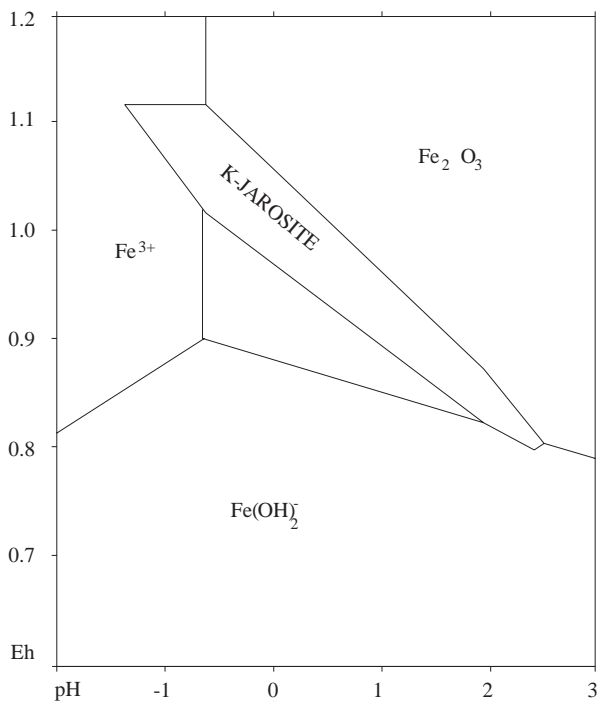


**Figure 3.** Stability region of K-jarosite at 298K (with the existence of Fe<sub>2</sub>O<sub>3</sub> and Fe(OH)<sub>2</sub><sup>-</sup>).

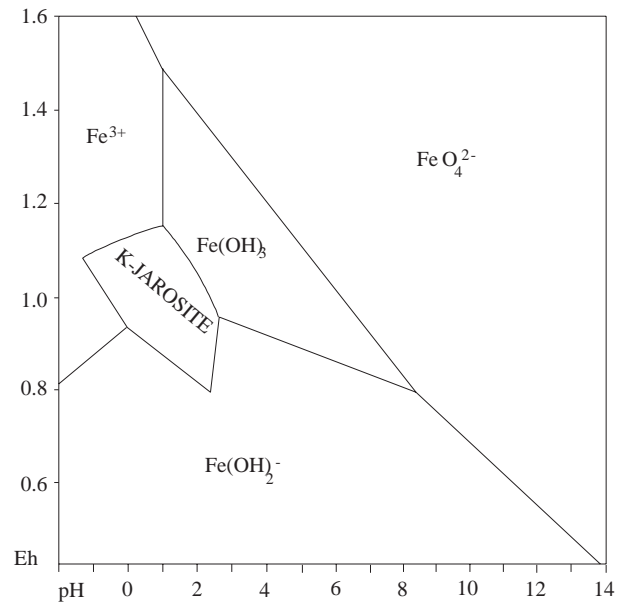


**Figure 4.** Stability region of K-jarosite at 298K (in absence of Fe<sub>2</sub>O<sub>3</sub>).

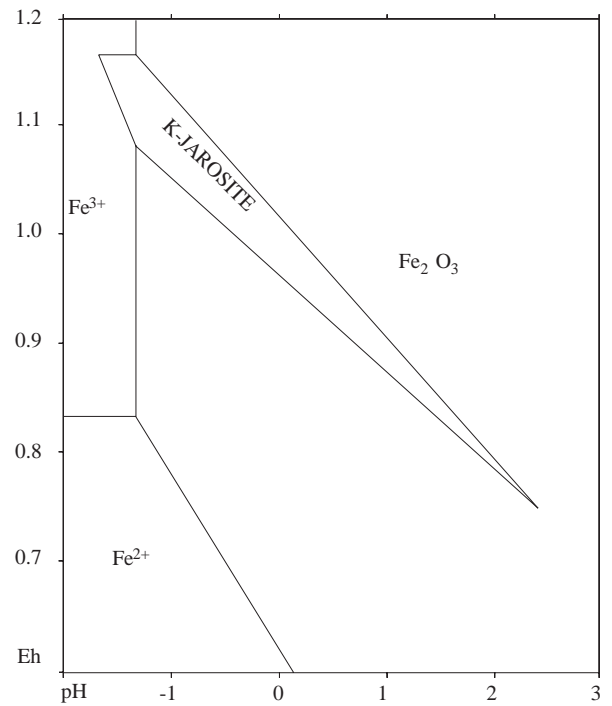


**Figure 5.** Stability region of K-jarosite at 368K (with the existence of Fe<sub>2</sub>O<sub>3</sub>).

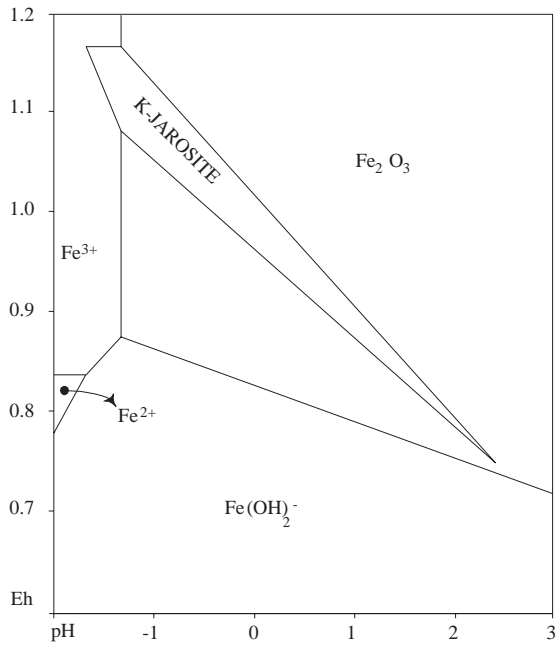


**Figure 6.** Stability region of K-jarosite at 368K (with the existence of  $\text{Fe}_2\text{O}_3$  and  $\text{Fe}(\text{OH})_2^-$ ).

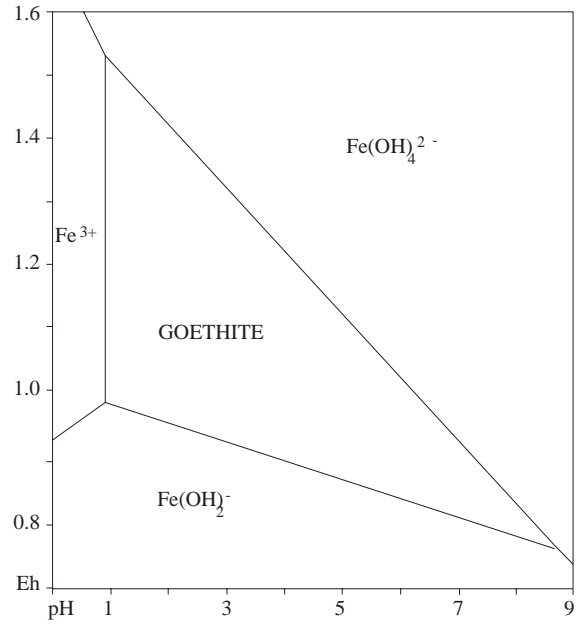


**Figure 9.** Stability region of Goethite at 298K (with the existence of  $\text{Fe}(\text{OH})_2^-$ ).

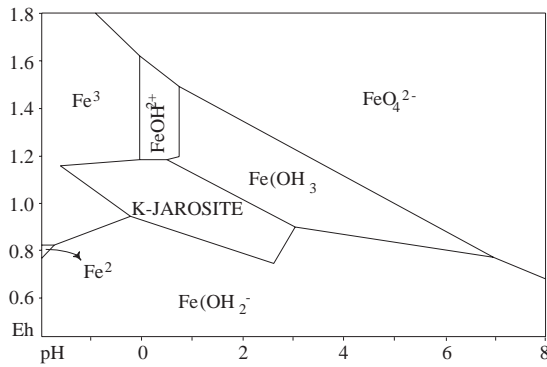


**Figure 7.** Stability region of K-jarosite at 368K (in absence of  $\text{Fe}_2\text{O}_3$ ).

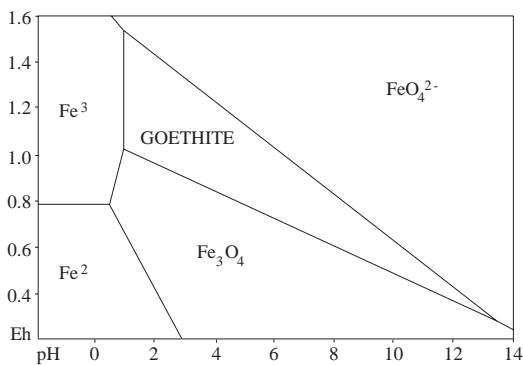


**Figure 8.** Stability region of Goethite at 298K (in absence of  $\text{Fe}_2\text{O}_3$  and  $\text{Fe}(\text{OH})_2^-$ ).

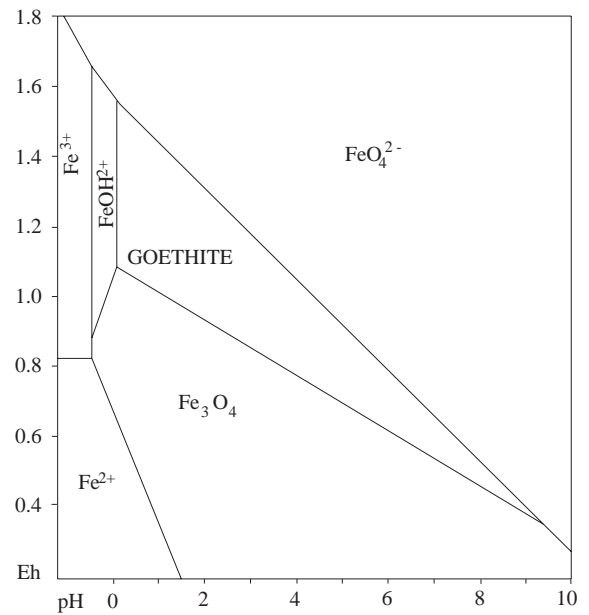


**Figure 10.** Stability region of Goethite at 368K (in absence of  $\text{Fe}_2\text{O}_3$  and  $\text{Fe}(\text{OH})_2^-$ ).

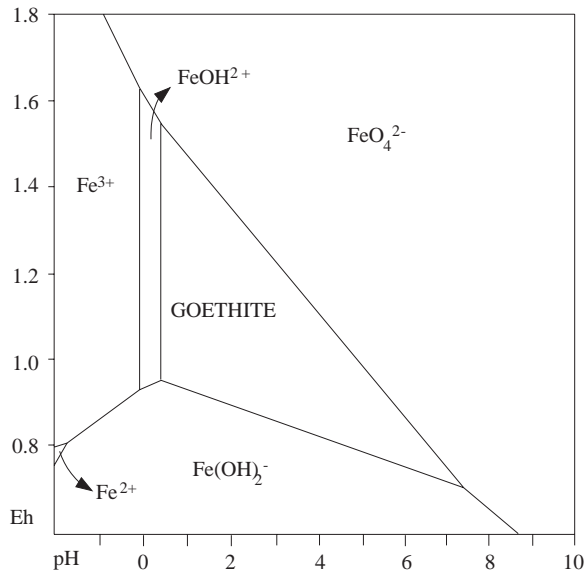


**Figure 11.** Stability region of Goethite at 368K (with the existence of  $\text{Fe}(\text{OH})_2^-$ ).

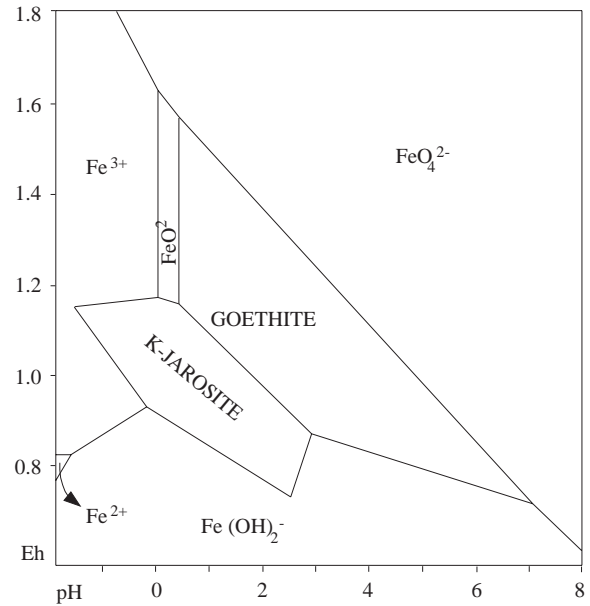


**Figure 13.** Stability regions of K-jarosite and Goethite at 368K (in absence of  $\text{Fe}_2\text{O}_3$ ).

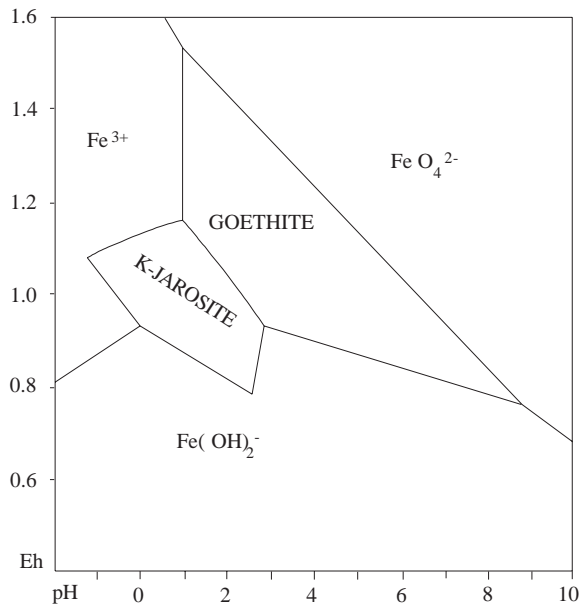


**Figure 12.** Stability regions of K-jarosite and Goethite at 298K (in absence of  $\text{Fe}_2\text{O}_3$ ).

### Conclusion

By comparing the Eh-pH diagrams for the jarosite stability region at 25 and 95°C (Figures 2 and 5, or 3 and 6, or 4 and 7), it can easily be seen that the field of jarosite not only shifts up to the area, that is more acidic and oxidizing but also becomes smaller as the temperature increases. These situations are also valid for goethite (Figures 8 and 10, or 9 and 11) and for the case where they both (jarosite and goethite) exist (Figures 12 and 13). Moreover, as can be seen, the stability field of jarosite (goethite as well) changes dramatically, depending upon the iron species taken into account. Consequently, the diagrams allow us to visualize the relative stability regions of the iron compounds with respect to iron precipitation. In addition to the thermodynamic considerations, however, reaction kinetics have an enormous importance in the precipitation of iron compounds.

### References

Acharya, S., Anand, S., and Das, R.P., "Iron Rejection through Jarosite Precipitation during Acid Pressure Leaching of Zinc Leach Residue", *Hydrometallurgy*, 31, 10-110, 1992.

Arauco, H., and Doyle, F.M., "Hydrolysis and Precipitation of Iron during Pressure Leaching of Zinc Sulphide Materials", *Hydrometallurgical Reactor*

Design and Kinetics, Eds. R.G. Bautista, R.J. Welsely, G.W. Warren, TMS, 187-207, 1986.

Arregui, V., Gordon, A.R., and Steintveit, G., "The Jarosite Process -Past, Present and Future", *Lead-Zinc-Tin '80*, Eds. J.M. Cigan, T.S. Mackey, and T.J. O'Keefe, TMS of AIME, 97-123, 1979.

- Austriana de Zinc S.A., US Patent 3,434,798; March 25, 1969.
- Barin, I., Knacke, O., and Kubaschewski, O., *Thermochemical Properties of Inorganic Substances – Plus Supplement*, Springer-Verlag, Berlin, 1977.
- Brown, J.B., “Jarosite-Goethite Stabilities at 25°C, 1 atm.”, *Mineral Deposita* (Berl.), 6, 245-252, 1971.
- Criss, C.M., and Cobble, J.W., “The Thermodynamic Properties of High Temperature Aqueous Solutions V”, *Journal of American Chemical Society*, 86, 5390-5393, 1964.
- Delvaux, R., “Lixiviation de Minerais de Zinc Grilles Selon le Procédé Goethite”, *Metallurgie* 16 (3), 154-163, 1976.
- Det Norske Zinkkompani: A/S, US Patent 3,434,947; March 25, 1969.
- Duby, P., “Graphical Representation of Equilibria in Aqueous Systems at Elevated Temperatures”, *High Temperature High Pressure Electrochemistry In Aqueous solutions*, NACE, 353-364, 1976.
- Dutrizac, J.E., “The Physical Chemistry of Iron Precipitation in the Zinc Industry”, *Lead-Zinc-Tin '80*, Eds. J.M. Cigan, T.S. Mackey and T.J. O'Keefe, AIME, New York, 532-564, 1980.
- Dutrizac, J.E., and Chen, T.T., “The Behaviour of Gallium During Jarosite Precipitation”, *Mineral Processing and Extractive Metallurgy Review*, 21, 16, 2000.
- Dutrizac, J.E., “The Effectiveness of Jarosite Species for Precipitating Jarosite”, *Journal of Metals*, 51, 12, 1999.
- Electrolytic Zinc Company of Australasia Ltd., US Patent 3,493,365; February 3, 1970.
- Garrels, R.M., and Christ, C.L., *Solutions, Minerals, and Equilibria*, Freeman, Cooper & Company, California, 1965.
- Hage, J.L.T., Schuiling, R.D., and Vriend, S.P., “Production of Magnetite from Sodium Jarosite under Reducing Hydrothermal Conditions. The Reduction of Fe(III) to Fe(II) with Cellulose”, *Canadian Metallurgical Quarterly*, 38, 4, 1999.
- Kellogg's Estimation, *Hydrometallurgy Class Notes* (Instructor: Prof. Dr. Paul F. Duby), HKSM Columbia University, 1988.
- Kershaw, M.G., and Pickering, R.W., “The Jarosite Process – Phase Equilibria”, *Lead-Zinc-Tin '80*, Eds. J.M. Cigan, T.S. Mackey and T.J. O'Keefe, AIME, New York, 565-580, 1980.
- Li, X.Z., and Hao, X.D., “New Construction Materials from Spanish Jarosite Processing Wastes”, *Mineral Engineering*, 12, 11, 1999.
- McAndrew, R.T., Wang, S.S., and Brown, W.R., “Precipitation of Iron Compounds from Sulphuric Acid Leach Solutions”, *CIM Bulletin*, 101-110, January 1975.
- NBS Tables of Chemical Thermodynamic Properties, *Journal of Physical and Chemical Reference Data*, 11, Supplement 2, 1982.
- Principe, F.T., and Demopoulos, G.P., “The Separation and Concentration of Iron from Zinc Process Solutions”, *Journal of Metals*, 51, 12, 1999.
- Sherritt-Gordon Mines Limited and Cominco Limited, “Process for the Treatment of Metal Sulphides for the Recovery of Non-Ferrous Metals”, *Belgian Patent No: 859857* (Canada 285,127 Aug 19, 1977), “Process for the Purification of Iron as Jarosite” *Belgian Patent No: 869,856* (Canada 28509 Aug 19, 1977).
- Societe de la Vieille Montagne, *Belgian Patent No: 724,214* (Nov. 20, 1968), *US Patent No: 3,652,264* March 28, 1972.
- Stumm, W., and Morgan, J.J., *Aquatic Chemistry*, 2<sup>nd</sup> Edition, John Wiley & Sons, New York, 753, 1981.
- Tsunoda, S., Maeshiro, I., Ewi, M., and Sekine, K., “The Construction and Operation of the Iijima Electrolytic Zinc Plant,” *AIME TMS*, paper no: A73-65, Chicago, 1973.
- Umetsu, Y., Tozawa, K., and Sasaki, K., “The Hydrolysis of Ferric Sulphate Solutions at Elevated Temperatures”, *Paper Presented at the CIM Conference*, August 22-26, 1976.